

Modelling Study of Magnetic Field's Effects on Solar Cell's Transient Decay

Senghane Mbodji¹, Martial Zoungrana², Issa Zerbo², Biram Dieng¹, Gregoire Sissoko³

¹Department of Physics, Alioune DIOP University of Bambey, Bambey, Senegal

²Laboratoire d'Energies Thermiques et Renouvelables (L.E.T.RE), Departement de Physique, U.F.R-S.E.A, Universite de Ouagadougou, Ouagadougou, Burkina Faso

³Laboratory of Semiconductors and Solar Energy, Department of Physics, Faculty of Science and Technology, Cheikh Anta Diop University, Dakar, Senegal

Email: gsissoko@yahoo.com

Received 19 October 2015; accepted 15 November 2015; published 18 November 2015

Copyright © 2015 by authors and Scientific Research Publishing Inc.

This work is licensed under the Creative Commons Attribution International License (CC BY).

<http://creativecommons.org/licenses/by/4.0/>



Open Access

Abstract

Experimental setup of transient decay which occurs between two steady state operating points is recalled. The continuity equation is resolved using both the junction dynamic velocity (S_f) and back side recombination velocity (S_b). The transient excess minority carriers density appears as the sum of infinite terms. Influence of magnetic field on the transient excess minority carriers density and transient photo voltage is studied and it is demonstrated that the use of this technique is valid only when the magnetic field is lower than 0.001 T.

Keywords

Solar Cell, Recombination Parameters, Magnetic Field

1. Introduction

Recombination parameters of solar cells are often investigated considering the steady state [1]-[4] or one of the many transient decay techniques [5]-[10]. As regards the transient states, we can cite the electroluminescence emission measurements [11], the frequency modulation approach [12], the open circuit voltage decay (OCVD) technique which is the most popular, the photocurrent decay (PCD) method [13], the stepped light-induced transient measurements of photocurrent and voltage (SLIM-PCV) [14], the microwave photocurrent decay (MW-PCD) [15], the well-known transient state operating between two steady state real operating points [16], etc.

The OCVD is usually combined to PCD method for determining, simultaneously, the lifetime and the considered surface recombination velocity (S) of materials and photovoltaic structures [13]. The SLIM-PCV is a valid

How to cite this paper: Mbodji, S., Zoungrana, M., Zerbo, I., Dieng, B. and Sissoko, G. (2015) Modelling Study of Magnetic Field's Effects on Solar Cell's Transient Decay. *World Journal of Condensed Matter Physics*, 5, 284-293.

<http://dx.doi.org/10.4236/wjcmp.2015.54029>

method to measure electron diffusion coefficient (D) and electron lifetimes of dye-sensitized solar cells (DCS) [14].

Respecting to the transient state operating between two steady state real operating points, it has been carried out on a solar cell placed in a fast-switch-interrupted circuit and submitted to a constant multispectral illumination. The transient decay occurs between two steady states through operating points depending on two variables resistors; this technique allows obtaining a transient decay at any operating point of the solar cell I-V curve (from the short circuit to the open one). By combining experimental and calculation results of the photo voltage transient decay response, the eigen value ω_0 of the fundamental decay mode and the decay time constant, the minority carrier lifetime (τ) is determined. The effective minority carrier diffusion length (L_{eff}), the junction dynamic velocity (Sf) and the backside recombination velocity (Sb) are then deduced [10]-[17].

Solar cells have seen remarkable improvements despite of some internal and external factors affecting their efficiency. Among internal factors, we can cite the grain boundary recombination velocity (S_{gb}) [1]-[3] [17], the intrinsic junction recombination velocity (S_{f_0}) [1]-[3] [8]-[10] [15] [17] related to the shunt resistance (R_{sh}) [2]-[18] due to losses at the junction, the series resistance (R_s) [2] [16] [18], and the back side recombination velocity (S_b) which quantifies the rate at which excess carriers are lost at the back surface of the solar cells [1]-[3] [8]-[10] [16] [17].

One of the external factors affecting efficiency of the solar cell, is the magnetic field which has various origins [19]. Depending on the position of the solar cell and the emitting source of the magnetic field, one can note some effects on the solar cells devices. That is why some works concerning influence of magnetic field on solar cells are done [12] [19] [20]. It is shown that, the peak power (P_m), the short-circuit photocurrent, the photo voltage and the solar cell diffusion capacitance which is reduced to the Shockley's depletion model decrease with the magnetic field when the solar cells is operating in steady state [21]. It has been also proved that under frequency modulation, the electron intrinsic mobility (μ), the diffusion coefficient (D), and the diffusion length (L) decrease when the silicon solar cell is both under applied magnetic field and frequency illumination mode [12].

In this present work, we are interesting of solar cell under magnetic field and in transient decay which occurs between two steady state operating points. We examine magnetic field effects on the eigenvalue ω_0 of the fundamental decay mode, the excess minority carriers and the photo voltage decay.

2. Materials and Methods

2.1. Experimental Setup and Working Principle of the Transient Decay Occurring between Two Steady State Operating Points

The experimental setup (Figure 1) includes a square signal generator (BRI8500) which pilots a Mosfet transistor type RFP50N06, two variables resistors R_1 and R_2 , a silicon solar cell submitted to a constant multispectral illumination, a digital oscilloscope, and a microcomputer.

The transient decay occurs according to the following procedure, described below.

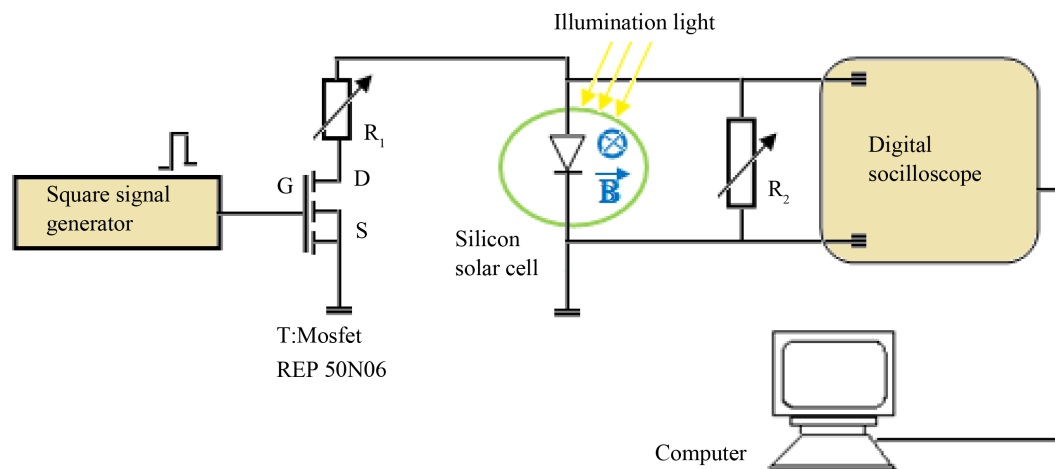


Figure 1. Experimental setup [10].

At time $t < 0$ the solar cell is in parallel with the resistor R_2 giving the potential V_2 corresponding to the steady state operating point F_2 . At time $t = 0$, the fast switch begins turning on and at time $t > 0$ is completely turned on. It then connects the resistor R_2 in parallel with the solar cell and the resistor R_1 . The voltage V_2 drops from V_2 to V_1 corresponding to the new steady state operating point F_1 as it can be seen on **Figure 2**.

This experience give an experimental photo voltage decay $V(t)$ which occurs between F_2 and F_1 . This experience is innovative because not involving light pulse and also does not consider only the open circuit photo voltage or the short-circuit photo current conditions as usually done in the OCVD and both the OCDV and PCD measurement techniques [13].

Figure 2 shows also how the I-V curves and then, the operating points are affected by the magnetic field as shown in [21].

2.2. Theory

A schematic diagram of the considered silicon solar cell under a magnetic field with its different coordinates is given in **Figure 3**.

The illumination was assumed to be uniform, such that the carrier generation rate depended only on depth (z) in the base and was expressed as:

$$G(z) = \sum_{i=1}^3 a_i \cdot \exp(-b_i z) \tag{1}$$

Coefficients a_i and b_i are deduced from modelling of the generation rate considered for over all the solar radiation spectrum [17].

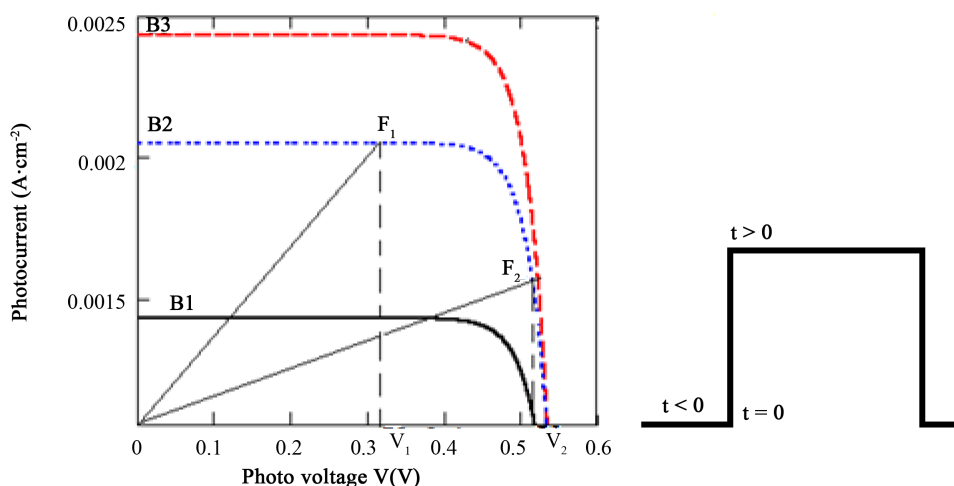


Figure 2. Illuminated I-V curve under constant magnetic field ($B_3 < B_2 < B_1$) with two specific operating points [9] [10].

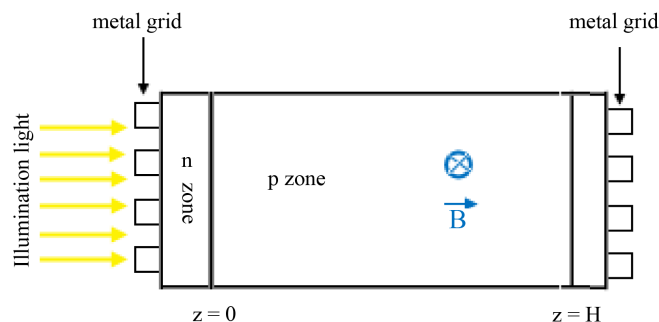


Figure 3. Illuminated silicon solar cell under magnetic field.

Also, the contributions of emitter and space charge region were neglected, the injection level is constant and the analysis was limited to the base region of thickness, $H = 200 \mu\text{m}$.

Hence, the transient excess minority carrier distribution $\delta(z, t)$ in the cell base was derived by solving the 1D continuity equation [10] [16]:

$$D^* \cdot \frac{\partial^2 \delta(z, t)}{\partial z^2} - \frac{\delta(z, t)}{\tau} = \frac{\partial \delta(z, t)}{\partial t} \quad (2)$$

where, the diffusion constant under magnetic field was expressed as [22]:

$$D^* = \frac{D}{1 + \mu^2 \cdot B^2}. \quad (3)$$

μ is the mobility of excess minority carriers in the base [22].

D and τ are respectively, solar cell minority carrier diffusion constant coefficient and carrier lifetime [10].

Equation (2) is resolved using below boundary conditions [1]-[3] [8]-[10] [16] [17]:

- At the junction, $z = 0$ (n-p interface):

$$D^* \cdot \frac{\partial \delta(z, t)}{\partial z} \Big|_{z=0} = Sf \cdot \delta(0, t). \quad (4)$$

- And at the back side of the silicon solar cell, $z = H$ [1]-[3] [8]-[10] [16] [17]

$$D^* \cdot \frac{\partial \delta(z, t)}{\partial z} \Big|_{z=H} = -Sb \cdot \delta(H, t). \quad (5)$$

Sf is defined as the Junction dynamic velocity [23]. It is the sum of two terms which traduce losses at junction and the collected excess minority carriers. Sf was called junction recombination velocity in our previous papers [1]-[3] [8]-[10] [16] [17] [22]. Sb is the back surface recombination velocity which traduces excess minority carriers lost at rear side of the solar cell [1]-[3] [8]-[10] [16] [17].

Equations (4) and (5) form a STURM Liouville's system of equations [9] whose solutions are separable variables of space and time. Thus, we can set:

$$\delta(z, t) = Z(z) \cdot T(t). \quad (6)$$

$Z(z)$ is the space function and $T(t)$, the time function are written, respectively:

$$Z(z) = A_1 \cdot \cos\left(\frac{z \cdot \omega}{\sqrt{D^*}}\right) + A_2 \cdot \sin\left(\frac{z \cdot \omega}{\sqrt{D^*}}\right) \quad (7)$$

and

$$T(t) = T(0) \cdot \exp\left[-\left(\omega^2 + \frac{1}{\tau}\right) \cdot t\right] \quad (8)$$

with: $\frac{1}{\tau_c} = \frac{1}{\tau} + \omega^2$, the decay time constant and where $\omega > 0$.

The boundary conditions give:

$$\beta = \frac{\omega \sqrt{D^*}}{Sf} = \frac{A_1}{A_2} \quad (9)$$

and

$$\text{tg}\left(\frac{H\omega}{\sqrt{D^*}}\right) = \frac{\omega \cdot \sqrt{D^*} (Sf + Sb)}{D^* \cdot \omega^2 - Sf \cdot Sb} \quad (10)$$

with:

$$\frac{\omega \cdot H}{\sqrt{D^*}} \in \left[0, \frac{\pi}{2} \left[\cup \right] \left(n - \frac{1}{2} \right) \pi; \left(n + \frac{1}{2} \right) \pi \right[\quad (11)$$

n is a natural number and:

$$\omega^2 \neq \frac{Sf \cdot Sb}{D^*} \quad (12)$$

Equation (10) is transcendental equation (of infinite number of positive roots), and was solved by Newton-Raphson numerical method [24] to obtain the allowed solutions ω_n . In other works which are based to OCDV method, solution from the work of Rose and Weaver [6] are adopted.

ω_0 is the eigenvalue of the fundamental decay mode and ω_n are the eigenvalues of the harmonic of order n decay mode, when $n > 0$.

Hence, we can see that A and B have discrete values and were finally calculated by normalization and Fourier transform [24]. Thus, the transient excess minority carriers density appears as the sum of infinite terms $\delta_n(z;t)$. Each term, $\delta_n(z;t)$, is the contribution of order n to the transient excess minority carriers density.

When n is equal to zero, we have the first term, $\delta_0(z;t)$, corresponding to fundamental mode which is characterized by ω_0 and when $n > 0$, $\delta_n(z;t)$ corresponds to harmonic of order n characterized by ω_n .

$\delta_n(z;t)$ is expressed as:

$$\delta_n(z,t) = Z_n(z) T_n(0) \exp\left(-\frac{1}{\tau_{c,n}} t\right) \quad (13)$$

The transient excess minority carriers density is:

$$\delta(z,t) = \sum_n \delta_n(z,t) \quad (14)$$

$\frac{1}{\tau_{c,n}} = \frac{1}{\tau} + \omega_n^2$ is discrete decay time constant.

The magnetic field effects on the eigenvalue of the fundamental decay mode and on the eigenvalues of the harmonic of order n decay mode are given on **Tables 1-3**.

Tables 1-3: range values of eigenvalue ω_0 of the fundamental decay mode, eigenvalues ω_n ($n > 0$) of the harmonic of order n decay modes and corresponding decay time constant modes:

We can note that, the eigenvalue ω_0 of the fundamental decay mode, the eigenvalues ω_n ($n > 0$) of the harmonic of order n decay mode decrease with the magnetic field, conversely, the different corresponding decay time constants modes increase with the magnetic field.

Table 1. $B = 0$ T.

n	0	1	2	3	4
ω_n ($s^{-1/2}$)	691	1409	2154	2918	3694
$\tau_{c,n}$ (μs)	1.430	0.450	0.200	0.110	0.070

Table 2. $B = 0.001$ T.

n	0	1	2	3	4
ω_n ($s^{-1/2}$)	502	1016	1544	2084	2630
$\tau_{c,n}$ (μs)	2.200	0.810	0.380	0.220	0.140

Table 3. $B = 0.01$ T.

n	0	1	2	3	4
ω_n ($s^{-1/2}$)	78	156	234	313	470
$\tau_{c,n}$ (μs)	4.380	4.050	3.610	3.120	2.250

3. Results and Discussion

3.1. Transient Excess Minority Carriers Density

For the simulation process, all the key equations were input into MathCAD software.

With base thickness and doping density fixed, the eigenvalues ω_n were determined by numerical solution of Equations (9) and (10) using Newton-Raphson method [23]. Compared to both OCDV and PCD techniques [13], where eigenvalues are calculated considering two operating points (open circuit and short-circuit), our method does not related to any operating point [10]-[16].

For the simulated modeling analyses, the transient excess minority carriers density was expressed as a function of magnetic field B , the junction dynamic velocity (Sf), the back side recombination velocity (Sb), the harmonic of order n , and the time (t).

Figures 4-6 show plots of the excess minority carriers density versus both the time and the magnetic field B which takes 0, 0.001 T and 0.01 T, respectively.

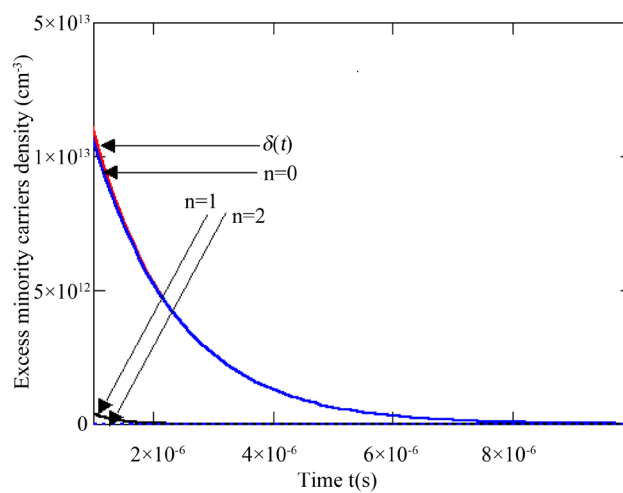


Figure 4. Excess minority carriers density versus the time $t(s)$ when the magnetic field $B = 0$ T with $H = 200 \mu\text{m}$, $D^* = 26 \text{ cm}^2 \cdot \text{s}^{-1}$, $\tau = 4.5 \mu\text{s}$, $\mu = 1000 \text{ cm}^2 \cdot \text{V}^{-1} \cdot \text{s}^{-1}$, $Sf = 4 \times 10^5 \text{ cm} \cdot \text{s}^{-1}$ and $Sb = 8 \times 10^3 \text{ cm} \cdot \text{s}^{-1}$.

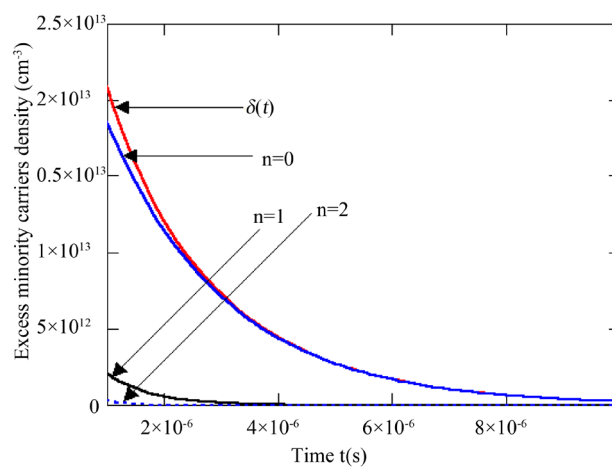


Figure 5. Excess minority carriers density versus the time $t(s)$ when the magnetic field $B = 0.001$ T with $H = 200 \mu\text{m}$, $D^* = 13 \text{ cm}^2 \cdot \text{s}^{-1}$, $\tau = 4.5 \mu\text{s}$, $\mu = 1000 \text{ cm}^2 \cdot \text{V}^{-1} \cdot \text{s}^{-1}$, $Sf = 3 \times 10^5 \text{ cm} \cdot \text{s}^{-1}$ and $Sb = 5 \times 10^3 \text{ cm} \cdot \text{s}^{-1}$.

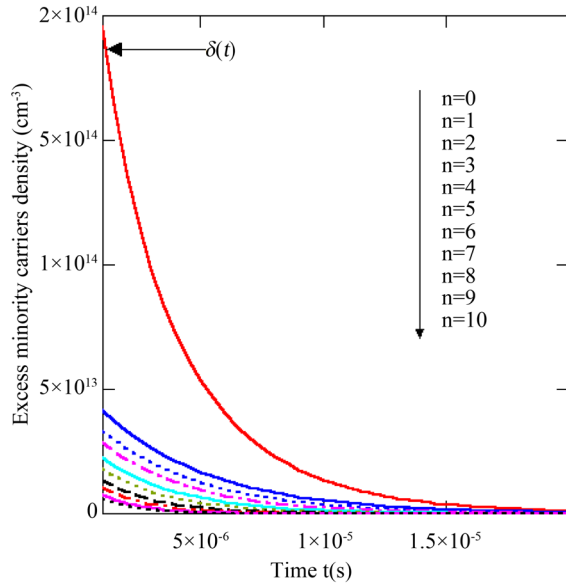


Figure 6. Excess minority carriers density versus the time $t(s)$ when the magnetic field $B = 0.01$ T with $H = 200 \mu\text{m}$, $D^* = 0.257 \text{ cm}^2 \cdot \text{s}^{-1}$, $\tau = 4.5 \mu\text{s}$, $\mu = 1000 \text{ cm}^2 \cdot \text{V}^{-1} \cdot \text{s}^{-1}$, $Sf = 2 \times 10^3 \text{ cm} \cdot \text{s}^{-1}$ and $Sb = 700 \text{ cm} \cdot \text{s}^{-1}$.

Without magnetic field, it has been remarked that the excess minority carriers density is obtained by the fundamental mode. The contributions of the harmonic of order n is neglected as found by [9] [10]-[16].

Figure 5 is the plot of the transient excess minority carriers density when $B = 0.001$ T.

When the applied magnetic field is $B = 0.001$ T, we noted two situations. The first is when $t < 2 \mu\text{s}$, the harmonics of order 1 and 2 aren't null but would be neglected while the fundamental mode reaches to the transient excess minority carriers density. When $t > 2 \mu\text{s}$, the transient excess minority carriers density is equal to the contribution of fundamental's mode.

In **Figure 6**, we show the variation of the transient excess minority carriers as the function of time when $B = 0.01$ T.

For $B = 0.01$ T, the excess minority carriers density cannot be taken to be equal to the contribution of the fundamental mode. The contribution of all terms are important.

Hence, for low magnetic field ($B < 10^{-3}$ T) we concluded that the transient excess minority carriers density is given by the contribution of the fundamental mode. Thus, the transient excess minority carriers density, at the junction, is expressed as:

$$\delta(t) = \delta_0(0, t) = Z_0(z)T_0(0) \exp\left(-\frac{1}{\tau_{c,0}} t\right). \tag{15}$$

For high values of magnetic field ($B > 10^{-3}$ T), the transient excess minority carriers density is calculated taking into account for all terms. So, both the OCDV and PCD method [13] which is used to determine the lifetime and the surface recombination velocity and the transient decay technique which occurs between two steady state operating conditions [9] [10]-[15] developed for investigation of recombination parameters wouldn't be valid in this range values of magnetic field.

3.2. Transient Photo Voltage Decay

Since the excess minority carrier density and the charge carriers gap ($\delta\phi$) at the junction are known, from the Boltzmann relation we can derive the photo voltage transient decay across the junction as:

$$V(t) = V_T \ln \left[\frac{\delta(0, t)}{\delta\phi} \cdot \exp\left(\frac{\Delta V}{V_T}\right) \right]. \tag{16}$$

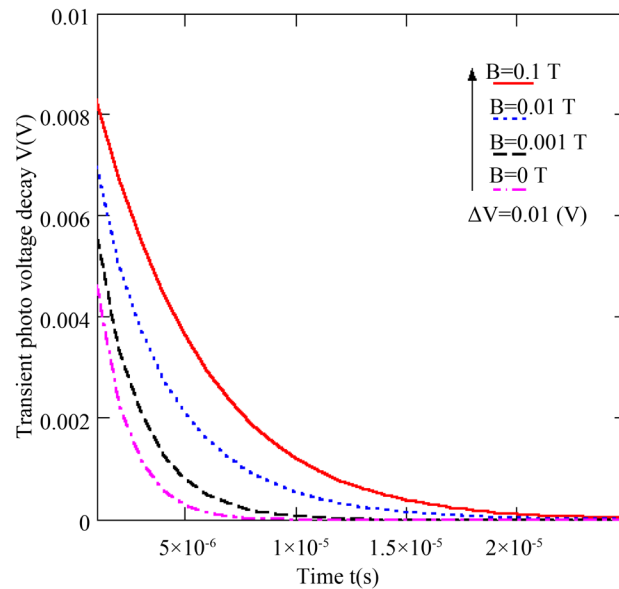


Figure 7. Transient photo voltage decay versus the time $t(s)$ with $H = 200 \mu\text{m}$, $\tau = 4.5 \mu\text{s}$, $\mu = 1000 \text{ cm}^2 \cdot \text{V}^{-1} \cdot \text{s}^{-1}$, and $\Delta V = 0.01 \text{ V}$.

$\delta\phi$ is charge carriers gap at the junction [10] and V_T is the thermal voltage.

The transient photo voltage decay was also simulated by analysing dependence on magnetic field. **Figure 7** shows plot of the transient photo voltage decay, at $H = 200 \mu\text{m}$, $\tau = 4.6 \mu\text{s}$ and $\Delta V = 0.01 \text{ V}$, with the magnetic field taking 0 T, 0.001 T, 0.01 T and 0.1 T, respectively.

In **Figure 7**, it is shown that, the transient photo voltage decay increases with magnetic field. The increase of magnetic field corresponds to low diffusion coefficient and diffusion length as demonstrated by [12]. Hence, excess minority carriers don't cross the junction and some of them are deflected leading to low transient photocurrent delivered by the solar cell as shown by [9].

4. Conclusions

The transient photo voltage decay occurring between two steady state operating points of a solar cell under magnetic field is studied. The corresponding experimental setup is recalled and the theoretical calculations of both the transient excess minority carriers density which is the sum of an infinite terms and photo voltage decay are made. Studies of effect of the magnetic field showed that eigenvalues decreased with magnetic field, conversely, to decay time constants which increased with magnetic field.

When the magnetic field B is lower than 0.001 T, the transient excess minority carriers density is equal to the contribution of the fundamental mode. The transient photo voltage decay can be used for the determination of recombination parameters. But for magnetic field greater than 0.001 T, the excess minority carriers density is the sum of all terms and the transient decay method is not recommended for the characterization of the solar cell.

References

- [1] Mbodji, S., Mbow, B., Barro, F.I. and Sissoko, G. (2011) A 3D Model for Thickness and Diffusion Capacitance of Emitter-Base Junction Determination in a Bifacial Polycrystalline Solar Cell under Real Operating Condition. *Turkish Journal of Physics*, **35**, 281-291.
- [2] Sissoko, G. and Mbodji, S. (2011) A Method to Determine the Solar Cell Resistances from Single I-V Characteristic Curve Considering the Junction Recombination Velocity (S_f). *International Journal of Pure and Applied Sciences and Technology*, **6**, 103-114.
- [3] Mbodji, S., Dieng, M., Mbow, B., Barro, F.I. and Sissoko, G. (2010) Three Dimensional Simulated Modelling of Diffusion Capacitance of Polycrystalline Bifacial Silicon Solar Cell. *Journal of Applied Science and Technology (JAST)*,

- 15, 109-114. <http://dx.doi.org/10.4314/jast.v15i1-2.54834>
- [4] Itturri-Hinojosa, A., Resendiz, M.L. and Torchynska, T.V. (2010) Numerical Analysis of the Performance of p-i-n Diode Microwave Switches Based on Different Semiconductor Materials. *International Journal of Pure and Applied Sciences and Technology*, **1**, 93-99.
- [5] Cuevas, A., Stocks, M., Macdonald, D. and Sinton, R. (1998) Applications of the Quasi-Steady-State-Photoconductance Technique. *Proceedings of 2nd World Conference and Exhibition on Photovoltaic Solar Energy Conversion*, 1236-1241.
- [6] Rose, B.H. and Weaver, H.T. (1983) Determination of Effective Surface Recombination Velocity and Minority Carrier Lifetime in High-Efficiency Si Solar Cells. *Journal of Applied Physics*, **54**, 238-247. <http://dx.doi.org/10.1063/1.331693>
- [7] Bitnar, B., Glatthaar, R., Marckmann, C., Spiegel, M., Tölle, R., Fath, P., Willeke, G. and Bucher, E. (1998) Lifetime Investigations on Screenprinted Silicon Solar Cells. *Proceedings of the 2nd World Conference and Exhibition on Photovoltaic Solar Energy Conversion*, 1362-1365.
- [8] Barro, F.I., Mbodji, S., Ndiaye, A.L., Zerbo, I., Madougou, S., Zougmore, F. and Sissoko, G. (2004) Bulk and Surface Parameters Determination by a Transient Study of Bifacial Silicon Solar Cell under Constant White Bias Light. *Proceedings of 19th European Photovoltaic Solar Energy Conference*, 262-265.
- [9] Mbodji, S., Mbow, B., Dieng, M., Barro, F.I. and Sissoko, G. (2010) A 3D Model for Thickness and Diffusion Capacitance of Emitter-Base Junction in a Bifacial Polycrystalline Solar Cell. *Global Journal of Pure and Applied Sciences*, **16**, 469-478.
- [10] Bocande, Y.L., Corréa, A., Gaye, I., Sow, M.L. and Sissoko, G. (1994) Bulk and Surfaces Parameters Determination in High Efficiency Si Solar Cells. *Proceedings of the World Renewable Energy Congress*, **3**, 1698-1700.
- [11] Lim, J., Kang, C., Kim, K., Park, I., Hwang, D. and Park, S. (2006) UV Electroluminescence Emission from ZnO Light-Emitting Diodes Grown by High-Temperature Radiofrequency Sputtering. *Advanced Materials*, **18**, 2720-2724. <http://dx.doi.org/10.1002/adma.200502633>
- [12] Diao, A., Thiam, N., Zoungrana, M., Sahin, G., Ndiaye, M. and Sissoko, G. (2014) Diffusion Coefficient in Silicon Solar Cell with Applied Magnetic Field and under Frequency: Electric Equivalent Circuits. *World Journal of Condensed Matter Physics*, **4**, 84-92. <http://dx.doi.org/10.4236/wjcmp.2014.42013>
- [13] Pisarkiewicz, T. (2004) Photodecay Method in Investigation of Materials and Photovoltaic Structures. *Opto-Electronics Review*, **12**, 33-40.
- [14] Nakade, S., Kanzaki, T., Wada, Y. and Yanagida, S. (2005) Stepped Light-Induced Transient Measurements of Photocurrent and Voltage in Dye-Sensitized Solar Cells: Application for Highly Viscous Electrolyte Systems. *Langmuir*, **21**, 10803-10807.
- [15] Schmidt, J. and Aberle, A.G. (1997) Accurate Method for the Determination of Bulk Minority-Carrier Lifetimes of Mono- and Multicrystalline Silicon Wafers. *Journal of Applied Physics*, **81**, 6186-6199. <http://dx.doi.org/10.1063/1.364403>
- [16] Barro, F.I., Seidou Maiga, A., Wereme, A. and Sissoko, G. (2010) Determination of Recombination Parameters in the Base of a Bifacial Silicon Solar Cell under Constant Multispectral Light. *Physical and Chemical News*, **56**, 76-84.
- [17] Diallo, H.L., Maiga, A.S., Wereme, A. and Sissoko, G. (2008) New Approach of both Junction and Back Surface Recombination Velocities in a 3D Modelling Study of a Polycrystalline Silicon Solar Cell. *The European Physical Journal Applied Physics*, **42**, 193-211. <http://dx.doi.org/10.1051/epjap:2008085>
- [18] El-Adawi, M.K. and Al-Nuaim, I.A. (2002) A Method to Determine the Solar Cell Series Resistances from a Single I-V Characteristic Curve Considering Its Shunt Resistance—New Approach. *Vacuum*, **64**, 33-36. [http://dx.doi.org/10.1016/S0042-207X\(01\)00370-0](http://dx.doi.org/10.1016/S0042-207X(01)00370-0)
- [19] Zerbo, I., Zoungrana, M., Ouedraogo, A., Korgo, B., Zouma, B. and Bathiebo, D.J. (2014) Influence of Electromagnetic Waves Produced by an Amplitude Modulation Radio Antenna on the Electric Power Delivered by a Silicon Solar Cell. *Global Journal of Pure and Applied Sciences*, **20**, 139-148. <http://dx.doi.org/10.4314/gjpas.v20i2.9>
- [20] Madougou, S., Made, F., Boukary, M.S. and Sissoko, G. (2007) I-V Characteristics For Bifacial Silicon Solar Cell Studied under a Magnetic Field. *Advanced Materials Research*, **18**, 303-312. <http://dx.doi.org/10.4028/www.scientific.net/AMR.18-19.303>
- [21] Madougou, S., Nzonzolo, Mbodji, S., Barro, I.F. and Sissoko, G. (2004) Bifacial Silicon Solar Cell Space Charge Region Width Determination by a Study in Modelling: Effect of the Magnetic Field. *Journal des Science*, **4**, 116-123.
- [22] Vardayan, R.R., Kerst, U., Wawer, P., Nell, M.N. and Wagemann, H.G. (1998) Method of Measurement of All Recombination Parameters in the Base Region of Solar Cells. *Proceedings of 2nd Conference and Exhibition on Photovoltaic Solar Energy Conversion*, Vienna, 6-10 July 1998, 191-193.

- [23] Madougou, S., Made, F., Boukary, M.S. and Sissoko, G. (2007) Recombination Parameters Determination by Using Internal Quantum Efficiency (IQE) Data of Bifacial Silicon Solar Cells. *Advanced Materials Research*, **18-19**, 313-324. <http://dx.doi.org/10.4028/www.scientific.net/AMR.18-19.313>
- [24] Goyal, M. (2007) *Computer-Based Numerical & Statistical Techniques*. Infinity Science Press, LLC, Hingham.